

Design of Maximum Thrust Plug Nozzles for Fixed Inlet Geometry

ROBERT P. HUMPHREYS,*
U.S. Air Force Academy, Colo.

AND

H. DOYLE THOMPSON† AND JOE D. HOFFMANN‡
Purdue University, Lafayette, Ind.

The calculus of variations is used to obtain the design equations for the contour of maximum thrust plug nozzles with a fixed inlet geometry and a specified geometric constraint. The optimum values of the injection angle at the throat and the cowl lip radius are determined by a parametric study. The problem is formulated to maximize the pressure thrust integral along the supersonic portion of the plug surface and includes the effect of base pressure. The analysis is carried out for irrotational flow and includes boundary-layer effects. A method is presented to determine if a given contour is an optimum, and a relaxation technique is used to obtain a solution to the resulting design equations. Numerical examples are presented for a fixed plug length and mass flow rate. The results of a parametric study to determine the optimum cowl lip radius and injection angle are presented and the resulting optimum nozzle is compared to one designed by Rao's Method. The importance of the transonic flow analysis and base pressure model are illustrated.

Nomenclature

a	= acoustic speed
C_{fi}	= incompressible skin-friction coefficient
E	= cowl lip location
F	= fundamental function, Eq. (7)
g	= general isoperimetric constraint
G	= boundary requirements, Eqs. (8), (9), and (10)
h_0	= annular half-height at the initial value surface
I	= functional to be maximized, Eq. (6)
\dot{m}	= mass flow rate
M	= Mach number
p_0	= total pressure
p	= static pressure
R	= gas constant
T	= thrust integral, Eq. (1)
u	= x component of velocity
v	= y component of velocity
V	= velocity modulus = $(u^2 + v^2)^{1/2}$
x	= spacial coordinate along the axis of symmetry
y	= spacial coordinate normal to the axis of symmetry
α	= Mach angle
β	= angle of inclination of the mean flow direction at the initial value surface to the axis of symmetry
γ	= ratio of specific heats
δ^*	= a boundary-layer thickness
δ'	= $\delta^* \cos \theta$
η	= inviscid core boundary
θ	= flow angle
λ_i	= Lagrange multipliers ($i = 1, 2, 3, 4$)
ρ	= density
ρ_d	= radius of curvature of the plug wall downstream of the initial value surface

τ = shear stress
 Φ = base pressure contribution to the thrust, Eq. (13)

Subscripts

b = base
 D = evaluated at point D
 DE = evaluated along the line DE
 E = evaluated at point E
 TD = evaluated along the boundary TD
 w = evaluated on the nozzle wall
 x = partial derivative with respect to x
 y = partial derivative with respect to y
 ∞ = freestream conditions

Other

(\cdot) = total derivative with respect to x

Introduction

CONCEPTUALLY, nonconventional nozzles such as the plug nozzle or the forced deflection nozzle offer advantages that cannot be achieved with conventional converging-diverging nozzles. The plug nozzle, for example, has the potential advantage of throttleability, thrust vector control, altitude compensation, and a shorter (and presumably lighter) nozzle for the same expansion ratio when compared with a conventional axisymmetric nozzle. Plug nozzles are currently operational on some jet engines and show considerable promise for rocket engine and scramjet applications. Because of its potential importance, the problem of maximizing the thrust of a plug nozzle is of considerable interest and is the subject of this paper.

The concept of applying optimization techniques to design thrust nozzles was introduced by Guderley and Hantsch¹ in 1955. Subsequently, Rao² simplified the analysis and developed a basic design procedure that has gained wide acceptance today throughout the industry. Rao also developed a formulation for the plug nozzle design problem,³ however, that formulation is limited to either a fixed length or, equivalently, a fixed expansion ratio, and further lacks the potential to be extended to include more general constraints or dissipative flows. More recently Guderley and Armitage⁴ formu-

Received January 7, 1971; presented as Paper 71-40 at the AIAA 9th Aerospace Sciences Meeting, New York, January 25-27, 1971; revision received April 29, 1971. This work has been partially sponsored by AFAPL, Wright-Patterson Air Force Base, Ohio, under contract number F33615-67-C-1068.

* Assistant Professor in the Department of Aeronautics. Member AIAA.

† Associate Professor of Mechanical Engineering, Associate Fellow AIAA.

‡ Associate Professor of Mechanical Engineering. Member AIAA.

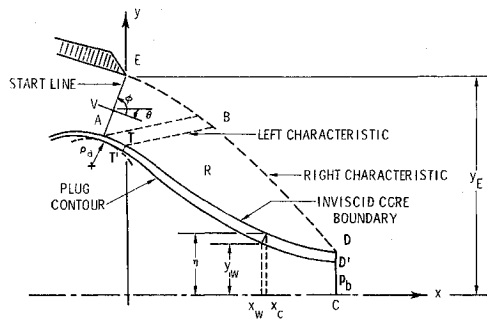


Fig. 1 Nozzle geometry and coordinate system.

lated the problem for the design of conventional axisymmetric nozzles using a more general approach which permits a selection of the geometric constraint. This additional flexibility was achieved only at the expense of a more complex problem formulation and an order of magnitude increase in the complexity of the numerical solution.

The additional potential of the Guderley-Armitage approach was realized when the method was extended by Hoffman and Thompson⁵ to include the effects of gas-particle flows, by Hoffman⁶ to include the effects of nonequilibrium reacting flows, and by Scofield, Thompson and Hoffman⁷ to include boundary-layer effects in the optimization. The essential difference in applying the method to these various types of flows is in the computation of the basic flowfield and not in the method itself.

The objective of this paper is to develop a design method for optimizing plug nozzles that can be extended to dissipative flows.

Problem Formulation

The plug contour to be optimized is that portion between points T' and D' , shown in Fig. 1 along with the remaining nozzle geometry. The cowl lip radius, y_E , and the mean flow direction at the initial value surface (injection angle), β , are prescribed, and the nozzle geometry and flowfield upstream of the characteristic BT are fixed. The resulting optimum contour is then the best for a given upstream geometry. The region R is assumed to be an inviscid core bounded by the streamline TD , the right characteristic DB , and the left characteristic BT . The streamline TD , denoted by $y = \eta(x)$, is separated from the plug surface by a boundary layer of thickness δ^* measured normal to the streamline. Thus, changes in the streamline TD will affect only the flow in region R .

The axial thrust to be maximized is obtained by summing the integrated pressure and shear forces on the plug $T'D'$ and the pressure forces acting on the plug base $D'C$, and expressing the resulting equation in terms of variables evaluated along TD . The thrust expression, developed in Ref. 8, is given by

$$T/2\pi = - \int_T^D [p(\eta - \delta') + \tau](\eta - \delta) dx + (\eta_D - \delta'_D)^2 p_b/2 \quad (1)$$

where $\delta' = \delta^* \cos \theta$ and (\cdot) denotes differentiation with respect to x . Equation (1) represents only that portion of the total axial thrust which is to be maximized in the variational problem. Any optimization, with respect to the injection angle and cowl lip radius must be accomplished by a parametric variation of those parameters. Since ambient pressure acts over the area πy_E^2 , the altitude for which the nozzle is designed is specified during the parametric study. Thus, it is desired to find the streamline $y = \eta(x)$ which maximizes Eq. (1) and from which the wall contour can be obtained. However, it is necessary to introduce certain constraints to assure that the results will be physically reliable.

The governing equations for axisymmetric, steady, isentropic, irrotational flow⁸ are the following:

$$(\gamma \rho u)_x + (\gamma \rho v)_y = 0 \quad (2)$$

$$u_y - v_x = 0 \quad (3)$$

where the subscripts x and y denote partial derivatives. Equation (2) is the continuity equation, and Eq. (3) is the irrotationality condition. The boundary TD is to be a streamline, which requires the dependent variables u and v to be related by $u\eta - v = 0$ along TD . This expression is multiplied by $\eta\rho$ for later convenience in algebraic manipulation. Thus

$$\eta\rho(u\eta - v) = 0 \quad \text{along } TD \quad (4)$$

In addition to these constraints, most engineering applications require the contour to have either a fixed length, a fixed surface area, or to be restricted geometrically in some other way. To place a physical limitation on the design, a general isoperimetric constraint of the following form is imposed:

$$\int_T^D g(\eta, \dot{\eta}, p) dx = \text{const} \quad \text{along } TD \quad (5)$$

A fixed length constraint is obtained by setting $g = 1$, and the condition for a fixed surface area is obtained by setting $g = (1 + \dot{\eta}^2)^{1/2}$.

The constraining relations given by Eqs. (2-5) are imposed on the thrust maximization by utilizing Lagrange multipliers. The functional to be optimized becomes

$$I = \iint_R F dy dx + \oint_{TDBT} G dx + \Phi \quad (6)$$

where

$$F = \lambda_1(u_y - v_x) + \lambda_2[(\gamma \rho u)_x + (\gamma \rho v)_y] \quad \text{in } R \quad (7)$$

$$G = -[p(\eta - \delta') + \tau](\eta - \delta) + \lambda_3 \eta \rho(u\eta - v) + \lambda_4 g \quad (8)$$

along TD

$$G = 0 \quad \text{along } DB \quad (9)$$

$$G = 0 \quad \text{along } BT \quad (10)$$

$$\Phi = (\eta_D - \delta'_D)^2 p_b/2 \quad \text{at } D \quad (11)$$

In the above equations λ_1 and λ_2 are functions of x and y , λ_3 is a function of x , and λ_4 is a constant.

The functional forms assumed for τ and δ' are $\tau = \tau(x)$ and $\delta' = \delta'(x)$. Since the flow is isentropic, the functional relations $p = p(u, v)$, $\rho = \rho(u, v)$, and $a = a(u, v)$ are valid. Thus, the dependent variables are the velocity components u and v .

The base pressure is taken as constant over the base of the plug at an effective value which is determined by the flow properties in the region R . Further, since the base pressure does not affect the flow properties in the region R , it must be treated in the variational problem as a constant which is not known a priori. As will be explained in more detail later, the optimum contour is approached in an iterative manner in which the value of the base pressure is recalculated in each iteration so that it is compatible with the flow properties. The optimization procedure is independent of the model used to calculate the base pressure. The particular model used in this investigation is given by the following empirical equation which is a curve fit of the data presented in Ref. 9:

$$p_b = 0.846 p/M^{1.3} \quad (12)$$

In addition, it is assumed that the stagnation temperature and pressure are known and are constant.

Necessary Conditions

In the calculus of variations there are certain necessary conditions arising out of the first variation of the functional which

§ The formulation of this problem for axisymmetric, steady, isentropic, rotational flow was also developed in Ref. 8.

have to be met for an extremal solution to exist. These conditions are the Euler equations, the transversality condition, the Erdman-Weierstrass corner condition for corner lines, and the corner condition for corner points on a boundary line. The Erdman-Weierstrass corner condition will not be investigated since flows in which corner lines arise are not to be considered. When the remaining conditions are satisfied it will be assumed on physical grounds that the resulting nozzle surface is indeed the maximizing solution.

The calculus of variations can be applied to Eq. (6) in order to determine the conditions necessary to an extremal solution. A detailed development of the results presented in the next few paragraphs can be found in Ref. 8. The necessary conditions are as follows:

Euler Equations

$$\lambda_{1y} + y\rho(1 - u^2)\lambda_{2x} - y\rho(uv/a^2)\lambda_{2y} = 0 \quad (13)$$

$$\lambda_{1x} + y\rho(uv/a^2)\lambda_{2x} - y\rho(1 - v^2/a^2)\lambda_{2y} = 0 \quad (14)$$

In the region of supersonic flow these equations are a system of hyperbolic, partial differential equations with characteristic directions which correspond to the characteristic directions of the basic flowfield. The compatibility equations are

$$d\lambda_1 \mp y\rho \operatorname{ctn}\alpha d\lambda_2 = 0 \quad (15)$$

Equation (15) is valid along the characteristics of the basic flowfield, which are the Mach lines defined by

$$dy/dx = \tan(\theta \pm \alpha) \quad (16)$$

The upper sign in Eqs. (15) and (16) refers to left-running characteristics and the lower sign to right-running characteristics.

Transversality Conditions

Along TD

Along this line variations in u , v , x , and y are treated as arbitrary and independent, which results in three equations:

$$\lambda_2 = \lambda_3 \quad (17)$$

$$\lambda_1 = \rho u(\eta - \delta')(\dot{\eta} - \dot{\delta}') + \lambda_4 \rho u g_p \quad (18)$$

$$\lambda_3 = (\eta - \delta')(du/dx + \dot{\delta}' dv/dx)/\eta - (\lambda_4/\eta) \times [g_p \dot{v} - (g_\eta - dg_\eta/dx)/(\rho u)] + \tau/(\eta \rho u) \quad (19)$$

Along DB

Along the exit characteristics, DB , variations in u , v , x , and y can be treated as arbitrary and independent. This results in two equations which can be combined to show that DB is a right-running characteristic along which the following equation must be satisfied:

$$\lambda_1 - \lambda_2 y \rho \operatorname{ctn}\alpha = 0 \quad (20)$$

Along BT

Since no variations in the gas properties or in x and y are allowed upstream of the left-running characteristic BT , the transversality condition is satisfied identically along this line.

Corner Conditions

Points B and T are considered to be fixed. Thus the corner condition is satisfied identically at these two points. The two conditions which must be satisfied at point D are:

$$[(\eta - \delta')(p\dot{\delta}' - \tau) - \lambda_4(g - \dot{\eta}g_\eta) + \lambda_3\eta\rho u\dot{\eta}]_{TD} = 0 \quad (21)$$

at D

$$[p(\eta - \delta') + \lambda_3\eta\rho u + \lambda_4g_\eta]_{TD} = (\eta_D - \delta'_D)p_b \quad \text{at } D \quad (22)$$

Rao's Result: A Special Case

It is of interest to note that the current formulation contains the results of Rao³ as a special case. If the axial length is held constant, then $g = 1$, and $g_p = g_\eta = g\dot{\eta} = 0$. Neglecting the wall shear stress and boundary layer thickness, Eq. (19), valid along TD , becomes $d\lambda_3/dx = du/dx$ or, since $\lambda_2 = \lambda_3$ on TD

$$\lambda_2 - \lambda_{2D} = u - u_D, \lambda_2 = \lambda_{2D} + V \cos\theta - V_D \cos\theta_D \quad (23)$$

Equation (18), which is also valid on TD , becomes

$$\lambda_1 = \eta\rho V \sin\theta \quad (24)$$

For any velocity distribution $u(x, y)$, $v(x, y)$ that satisfies the flow equations, the two pairs of functions: $\lambda_1 = \text{const}$, $\lambda_2 = \text{const}$, and $\lambda_1 = y\rho V \sin\theta$, $\lambda_2 = V \cos\theta$, satisfy the partial differential Eqs. (13) and (14) which are valid throughout the flowfield. Thus, Eqs. (23) and (24) must also be valid along DB where Eq. (20) applies. Substitution of Eqs. (23) and (24) into Eq. (20) yields, $y\rho V \sin\theta - y\rho \operatorname{ctn}\alpha(\lambda_{2D} + V \cos\theta - V_D \cos\theta_D) = 0$, which reduces directly to

$$V \cos(\theta + \alpha)/\cos\alpha = \text{const} \quad (25)$$

Equations (15) and (20) can be combined to yield $\lambda_1 = (Cy\rho \operatorname{ctn}\alpha)^{1/2}$ where C is a constant. Substituting this into Eq. (24) yields

$$y\rho V^2 \sin^2\theta \tan\alpha = \text{const} \quad (26)$$

Equations (25) and (26) must be satisfied along the exit characteristic DB and are identical to the equations obtained by Rao. At point D , Rao obtained the corner condition

$$(p - p_b) \operatorname{ctn}\alpha/(\rho V^2/2) = -\sin 2\theta \quad \text{at } D \quad (27)$$

This equation can also be obtained by neglecting the wall shear and boundary-layer thickness in Eqs. (18) and (22) and by substituting Eqs. (17) and (18) into Eq. (20). This results in

$$\lambda_3 = v/\operatorname{ctn}\alpha \quad (28)$$

which must be satisfied at point D . This result is then substituted into the corner condition, Eq. (22), which reduces directly to Eq. (27).

Computer Program

The problem formulated here was programmed in FORTRAN IV for the IBM 7094 and CDC 6500 computers. In the program the boundary-layer thickness δ^* is assumed to be zero. Correction for boundary-layer thickness can be made to the optimized contour by using the displacement thickness to adjust the wall coordinates. The numerical techniques, including the method of contour modification, are discussed in the next section.

Numerical Methods

Solution Procedure

The solution procedure consists of estimating what the optimum contour should be, analyzing the contour to see if it is an optimum, and modifying the contour if it is not an optimum. This indirect method is in contrast to the Rao³ technique in which optimum contours are constructed directly by calculating the flowfield backwards from the last right-running characteristic which is obtained, for a given plug length and mass flow rate, by solving a two-point boundary-value problem. No direct method has been found for the present analysis.

In order to analyze the contour it is necessary first to solve the flowfield by the method of characteristics which requires an initial value line. The start line either can be read in from data cards or generated internally. The internally generated start line is obtained from either a modified Moore-Hall¹⁰

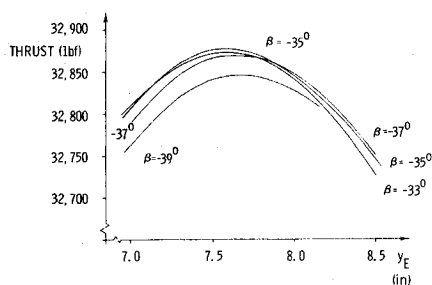


Fig. 2 Thrust vs cowl lip radius.

transonic flow analysis or an isentropic flow analysis in which the Mach number is assumed to be constant along a straight line. The details of the Moore-Hall analysis and the necessary modifications are developed in Ref. 8. In any case, the start line will always be from point *A* to point *E* shown in Fig. 1.

Before going into the details of the numerical procedure, the conditions at point *T* (see Fig. 1) need to be examined. For zero boundary-layer thickness the contour *TD* coincides with *T'D'*. In the problem formulation, point *T* was considered to be fixed and thus variations in the plug contour are allowed only downstream of point *T*. In carrying out the iterative optimization process, the contour downstream of point *T* is modified and consequently, a sharp corner can arise at point *T*. In order to avoid this sharp corner, it is necessary to specify the plug curvature in this region. The actual nozzle will then be forced to follow this contour up to a fixed, but not predetermined, point. As a result, point *T* is located so that no discontinuity in the plug contour arises as the contour modification is carried out. Point *B* is then located along the left characteristic originating at point *T*. In general, point *T* will always be downstream from point *A* and can never move upstream of point *A* during the contour modification process. The calculation of the flowfield is carried out in recognition of this situation.

First, the flowfield is obtained by the method of characteristics which is initiated from the start line *AE*. The characteristics have directions given by Eq. (16), and the compatibility relations valid along these lines are

$$d\theta \mp \cot \alpha dV/V \pm [(\sin \theta \sin \alpha)/y \sin(\theta \pm \alpha)] dy = 0 \quad (29)$$

The upper signs refer to left-running characteristics and the lower signs to right-running characteristics. Once the flowfield is known, Eqs. (17), (21), and (22) can be used to solve for λ_1 and λ_2 at point *D*.

Starting from point *D*, Eqs. (17), (18), and (20) can be used to evaluate λ_1 and λ_2 along *TD*. The plug surface *TD* then serves as an initial-value line from which to initiate the method of characteristics solution for λ_1 and λ_2 in the region *R*. These two multipliers have the same characteristic directions as the flowfield, and their compatibility relations are given by Eqs. (15).

Equation (20) must be satisfied along the exit characteristic, *DB*, and serves as a check to determine whether or not a given contour is an optimum. In general, Eq. (20) will not be satisfied by the first guess for the optimum surface and it is then necessary to calculate a new wall contour. In calculating the new contour it is convenient to consider Eq. (20) as an error function such that

$$E = \lambda_1 - \lambda_2 p \cot \alpha \quad \text{along } DB \quad (30)$$

Changes in the wall contour are designed to drive *E* to zero as rapidly as possible and upon this premise a new wall is constructed. This method of contour modification is a relaxation technique, and was developed by Scofield, Thompson, and Hoffman.⁷ The details of the method are described in the next section.

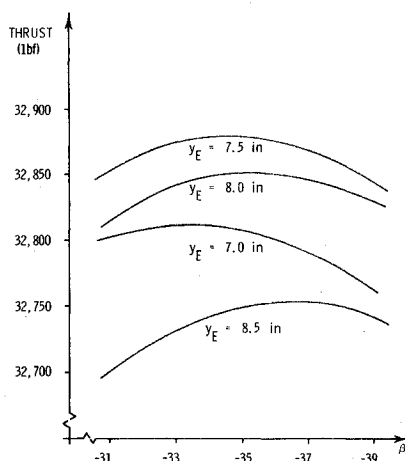


Fig. 3 Thrust vs injection angle.

After the new wall contour is obtained, the above procedure is repeated. This iteration procedure continues until the error function *E* is reduced to an acceptable value near zero.

Relaxation Technique

The wall modification procedure or wall relaxation must, above all, produce rapid convergence. The entire procedure is designed with this in mind. In order to change the wall contour it must first be determined how changes in the contour affect the error function given by Eq. (30). To do this, the wall angle θ is chosen as the independent variable and the error function *E* as the dependent variable. Theoretically the wall angle can be perturbed at a point on the wall, the flowfield and Lagrange multiplier field recalculated, and the change in the error function along *DB* evaluated. This procedure could be repeated until every wall point had been perturbed and the corresponding changes in the error function found. This would result in an $n \times n$ matrix (n = number of wall points) relating changes in the wall angle to changes in the error function. This can be written in partial derivative form as

$$\partial E_i / \partial \theta_j = (E_i - E_{i0}) / (\theta_j - \theta_{j0}) \quad (i, j = 1, \dots, n) \quad (31)$$

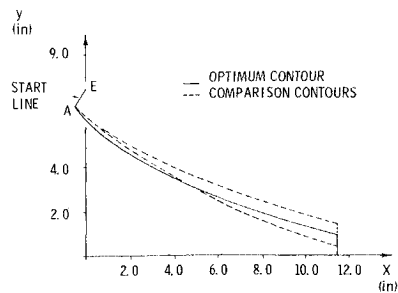
where E_{i0} and θ_{j0} are the initial values of E_i and θ_j .

Once these partial derivatives are known, a truncated Taylor series could be used to relate changes in the wall angle

Table 1 Parametric study results

Injection angle, deg	Cowl lip radius, in.	Thrust, lbf
-31.00	7.00	32,803
-31.00	7.50	32,853
-31.00	8.00	32,813
-31.00	8.50	32,699
-33.00	7.00	32,811
-33.00	7.50	32,874
-33.00	8.00	32,842
-33.00	8.50	32,731
-35.00	7.00	32,808
-35.00	7.50	32,877
-35.00	8.00	32,846
-35.00	8.50	32,747
-37.00	7.00	32,791
-37.00	7.50	32,869
-37.00	8.00	32,847
-37.00	8.50	32,753
-39.00	7.00	32,763
-39.00	7.50	32,844
-39.00	8.00	32,829
-39.00	8.50	32,741
-34.00	7.55	32,881

Fig. 4 Optimum contour.



to changes in the error function such that

$$E_i - E_{i0} = (\partial E_i / \partial \theta_j)_{\theta_{j0}} (\theta_j - \theta_{j0}) \quad (i, j = 1, \dots, n) \quad (32)$$

The repeated subscript j in Eq. (32) indicates a summation. Since the desired value of the error function is zero, Eqs. (32) could be used to solve for the value of the wall angle that will drive the error function to zero. Thus,

$$-E_{i0} = (\partial E_i / \partial \theta_j)_{\theta_{j0}} \Delta \theta_j \quad (i, j = 1, \dots, n) \quad (33)$$

In theory Eq. (33) could be solved, but in practice this could be difficult and time consuming when a large number of wall points are involved.

In their investigation of the problem for conventional nozzles, Scofield, Thompson, and Hoffman⁷ found that it could be assumed that there is a direct relationship between changes in the wall angle and changes in the error function which lie on the same right-running characteristics. That is, the major effect on E due to a change in the wall angle at a point propagates down the right-running characteristic which originates at that point. This same type of assumption was found to be valid for the plug nozzle when applied along left-running characteristics originating at the wall. Thus, Eqs. (33) reduce to n simple independent equations which can be solved for $\Delta \theta$ at each of the n wall points.

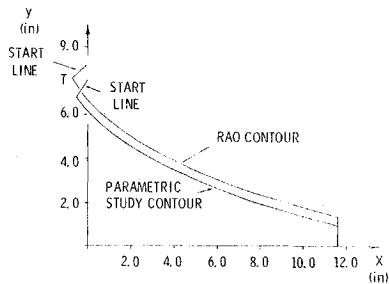
$$\Delta \theta_i = -E_{i0} / (\partial E_i / \partial \theta_i) \quad (i = 1, \dots, n) \quad (34)$$

Since the problem is nonlinear, the final solution must be approached iteratively. The wall angles for the $(r + 1)$ iteration are given by

$$\theta_i^{(r+1)} = \theta_i^r + \Delta \theta_i \quad (i = 1, \dots, n) \quad (35)$$

The procedure just described is a simple method of adjusting the wall contour but would require considerable time if carried out in all of its detail. Scofield, Thompson, and Hoffman⁷ used two methods to reduce the computer time and both

Fig. 5 Contour comparison.



are used in the current investigation. First, it was noted that a nearly linear relationship exists between the partial derivatives $\partial E_i / \partial \theta_i$ and the corresponding wall axial coordinate x . Because of this linear relationship it is possible to calculate the partial derivatives at a few points (typically ten) and then fit a straight line through these points by the method of least squares. The remaining partial derivatives can be taken from the fitted straight line, thereby reducing the time required for calculating $\partial E_i / \partial \theta_i$. Second, the partial derivatives were recalculated only after several iterations rather than after each iteration.

Results

The problem formulation assumes specified values for the cowl lip radius and initial injection angle. Since both of these parameters have a significant influence upon the total thrust of plug nozzles, it may be desirable, in some cases, to determine the optimum values of these parameters. To illustrate how this can be done, a parametric study was carried out to determine the optimum cowl lip radius and injection angle for a given length nozzle. The purpose of this section is to present the results of such a parametric study and to compare the optimum nozzle to one designed by Rao's method⁸ for the same mass flow rate and ambient pressure. The importance of the transonic flow analysis and the base pressure calculations are also illustrated.

Parametric Study to Determine the Optimum Cowl Lip Radius and Injection Angle

As mentioned previously, the thrust maximized in the variational problem does not represent the total axial thrust. The total thrust is given by the equation

$$T/2\pi = \int_A^E [p + \rho V^2 \sin(\phi - \theta) \cos \phi / \sin \theta] y dy - y^2_E p_a / 2 - \int_A^D [p y + \tau] y dx + y_D^2 p_b / 2 \quad (36)$$

where the angles ϕ and θ are shown in Fig. 1. The last two terms in Eq. (36) are obtained by neglecting the boundary-layer thickness in Eq. (1). The first term accounts for the pressure and momentum forces acting across the initial-value line EA , the second term accounts for the ambient pressure acting on the frontal area of the inlet, the third term is the pressure thrust generated by the plug contour, and the last term is the plug base thrust. The cowl lip radius and injection angle influence the first two terms, while the contour optimization is used to maximize the last two terms for a specific choice of cowl lip radius and injection angle. However, as explained earlier, the radius of curvature of the plug between points A and T is specified a priori, and as a result, this portion of the nozzle wall will not necessarily be an optimum. Thus, the plug contour generated by the present technique yields a thrust maximum for the specified inlet radius of curvature, injection angle, and cowl lip radius. To determine the best over-all nozzle when no constraints are placed on the cowl lip radius and injection angle, these two parameters can be varied parametrically and the optimum plug con-

Table 2 Coordinates of the optimum plug contour

x , in.	y , in.	θ° , deg
-0.56069	6.71874	-36.25027
-0.55023	6.71087	-37.75027
-0.53999	6.70272	-39.25027
-0.52996	6.69430	-40.75027
-0.52016	6.68563	-42.25027
-0.51059	6.67670	-43.75027
-0.50125	6.66753	-45.25027
-0.49216	6.65811	-46.75027
-0.48331	6.64846	-48.25027
-0.40216	6.55777	-48.02999
-0.29091	6.43493	-47.64577
-0.03515	6.15846	-46.81925
0.29695	5.81595	-44.30856
0.99456	5.21035	-37.84839
2.10220	4.45395	-31.24354
3.01742	3.93915	-27.61354
5.08714	2.98654	-22.22618
6.75042	2.35672	-19.37574
8.85315	1.67387	-16.70496
11.51707	0.95441	-13.26458

tour can be obtained for each set of these parameters. The maximum thrust nozzle is then selected from this group of nozzles. Such a parametric study is presented in this section.

The parametric study was conducted for a nozzle which has a mean radius of curvature at the throat of 0.705 in., a downstream radius of curvature of 0.5 in., and a length from point *T* to point *D* (see Fig. 1) of 12.0 in. The mass flow rate, ambient pressure, and incompressible skin-friction coefficient were selected as $\dot{m} = 148.08$ lbm/sec, $p_a = 14.7$ psia, and $C_{fi} = 0.002$, respectively. The engine was assumed to operate with a chamber pressure of 500.0 psia and a chamber temperature of 6000.0°R. The exhaust products were assumed to have a gas constant of 56.0 (ft-lbf)/(lbm-°R) and a ratio of specific heats of 1.23. The base pressure was calculated using Eq. (12) and the wall shear stress by using

$$\tau = C_{fi}\rho V^2/2 = C_{fi}\rho V^2/[2 + 0.72(\gamma - 1)M^2] \quad (37)$$

where the expression for the local skin friction coefficient, C_{fi} , was obtained from Ref. 11. Equation (37) was used to calculate τ along the wall once the flowfield was calculated, and the function $\tau(x)$ assumed earlier is obtained by a curve fit of those results. The nozzle was designed for a subsonic burning engine, thus a modified Moore-Hall⁹ start line was used. As the cowl lip radius and injection angle are changed, the throat height is varied in order to keep the mass flow rate constant. A total of 20 computer runs were made to determine the optimum cowl lip radius and injection angle. The results of these runs are presented in Table 1.

The data in Table 1, except the last set where $\beta = -34^\circ$ and $y_E = 7.55$ in., are plotted in Figs. 2 and 3. Figure 2 is a plot of thrust as a function of cowl lip radius with the injection angle as a parameter, and Fig. 3 is a plot of thrust as a function of injection angle with the cowl lip radius as a parameter. From Fig. 2, it was determined that the optimum cowl lip radius would be approximately 7.55 in., and the optimum injection angle was determined from Fig. 3 to be approximately -34° . One final computer run was made using these values for the cowl lip radius and injection angle. This run resulted in a thrust of 32,881 lbf, which is the maximum of the total of 21 designs. The coordinates and slopes of the resulting optimum contour are given in Table 2 and plotted in Fig. 4. Two other contours of the same length have also been plotted in Fig. 4 for comparison to the optimum. One contour is 0.5 in. above the optimum at point *D* and the other is 0.5 in. below the optimum at the same point. As expected, both contours produce a lower thrust than the thrust of the optimum contour, the upper contour producing a thrust of 32,556 lbf, and the lower contour producing 32,601 lbf.

Thus, it is possible to determine the optimum values for both the cowl lip radius and injection angle even though these quantities were fixed in the variational problem formulation. This approach to the problem is also useful in cases where either the cowl lip radius or injection angle are dictated by other considerations. This situation could arise, for example, where the cowl lip radius is limited by the vehicle size but no restrictions are placed on the injection angle. The best injection angle for the given cowl lip radius could be obtained from a study such as illustrated in Fig. 3.

Comparison to Rao Nozzles

Since the current formulation contains the results of Rao³ as a special case, it is of interest to compare the nozzles designed by the two methods.

Rao results

The design equations obtained by Rao were programmed in order to compare his technique with the current formulation. A comparison was made with the same mass flow rate, plug length, ambient pressure, thermodynamic properties, and base pressure model as those employed in the parametric

study. The Rao method yielded an optimum cowl lip radius of 8.33 in. and an optimum injection angle of approximately -58.5° with a resulting thrust of 34,253 lbf. The coordinates and slopes of the resulting optimum contour are given in Table 3 and plotted in Fig. 5. By comparing the data in Table 3 with that in Table 2, it can be seen that the contour obtained by Rao's method lies above the contour obtained from the parametric study. In order to compare the shapes of these two contours, the contour which resulted from the parametric study was also plotted in Fig. 5. As can be seen from Fig. 5, the two contours are almost identical in shape except in the throat region, the most significant difference being in the injection angle and cowl lip radius. Since the start line or sonic line assumptions for these two models are not the same, it was suspected that the differences in the results were caused by the dissimilarities in the start lines. The results of an investigation to determine if this was indeed the case are presented in the next section.

Importance of start line

Since Rao assumed a linear sonic line along which the flow direction is constant, an attempt was made to duplicate his results by using such a start line along which the Mach number was slightly greater than unity. The cowl lip radius and injection angle were fixed at the values found for the optimum Rao nozzle and the wall shear stress was set equal to zero since Rao did not account for this in his formulation. The general flow condition produced by a parallel uniform flow with the flow direction toward the axis of symmetry is one of compression. Unless the Mach number along the start line is increased to approximately 1.5, the compression results in subsonic Mach numbers in the throat region. However, the assumption of a Mach number greater than one along the start line implies that the flow has passed through the minimum area and should be expanding. This requires the flow direction to become more negative along the start line, *EA*. By linearly decreasing the flow direction by 6° along the start line from top to bottom, the compression problem was eliminated. For the contour discussed here, the flow direction at point *E* was fixed at -56.0° and decreased uniformly to -62.0° at point *A*. The resulting plug contour matched the Rao contour reasonably well but the thrust was approximately 2700 lbf lower.

One final attempt was made to duplicate Rao's results. A right-running characteristic near the throat was taken from the Rao nozzle flow field and used as a start line for the present analysis. This start line produced a contour almost identical to Rao's and the thrust was 34,373 lbf compared to 34,375 lbf

Table 3 Coordinates of the Rao contour

x , in.	y , in.	θ° , deg
-0.63971	7.60953	-60.69463
-0.52553	7.41133	-59.26745
-0.38991	7.19374	-56.76264
-0.28105	7.03417	-54.62384
-0.11511	6.81327	-51.56682
0.08454	6.57580	-48.37210
0.26305	6.38348	-45.92900
0.54982	6.10414	-42.64770
0.80980	5.87499	-40.18842
1.11665	5.62702	-37.74413
1.75877	5.16641	-33.72519
2.24216	4.85831	-31.35732
3.03421	4.40556	-28.40556
4.04195	3.89898	-25.23198
5.33714	3.33063	-12.27169
6.55991	2.85772	-20.07902
8.07079	2.33921	-17.86199
9.28531	1.96623	-16.29294
11.51781	1.37506	-13.25333

for Rao's nozzle. Thus, when compatible start lines are employed, the two techniques yield the same results.

These results indicate that the start line model is very important in the design of optimum plug nozzles, and approximations in this region should be carefully evaluated.

Effect of the Base Pressure Model

Another possible source of error in plug nozzle design is in the base pressure model. The importance of the base pressure model is illustrated in this section.

After the parametric study was completed and the optimum nozzle determined, the equation used to calculate the base pressure was changed from Eq. (12) to

$$p_b = p_\infty [1 - 0.715\gamma(M_\infty^{2.3} - 0.92M_\infty^2 - 0.03)/M_\infty^{2.7}] \quad (38)$$

which was obtained from Ref. 12. This equation produces values of base pressure considerably higher than Eq. (12). The primary objective in using Eq. (38) was to determine the effect of the base pressure model on nozzle performance and contour. All other parameters were set at the values used for the parametric study, and the cowl lip radius and injection angle were set at their optimum values of 7.55 in. and -34° . The coordinates and slope of the resulting contour are given in Table 4 and plotted in Fig. 6. The contour obtained from the parametric study is also plotted in Fig. 6. As can be seen from this figure, the base pressure model has a considerable effect upon the shape of the plug contour. The base height, y_D , increased from 0.954 in. to 2.34 in. and the wall slope at point D increased from -13.26° to -3.08° . In addition, the thrust increased to 32,965 lbf because of the higher base pressure. Since the thrust has changed, it is expected that the optimum cowl lip radius and injection angle will also be different. Thus, in addition to a direct change in the thrust contribution of the plug base, the base pressure model significantly influences the shape of the optimum contour.

Summary

An analysis and computer program have been developed for the optimization of plug nozzle contours with boundary layer shear stress accounted for in the optimization. The solution makes no particular assumption about the upstream nozzle geometry but simply requires the flow conditions along a start line to be available in order to initiate the flowfield solution. The problem was formulated for irrotational flow. A general isoperimetric constraint was imposed upon the plug contour in the region of supersonic flow. A complete set of

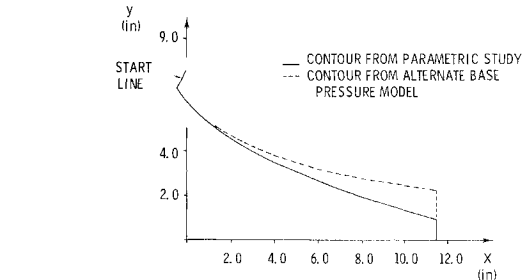


Fig. 6 Optimum contour for alternate base pressure model.

partial differential equations with sufficient boundary conditions was obtained for determining the flow properties and Lagrange multipliers. A method was presented to determine if a given contour is an optimum, and a relaxation technique was used to obtain a solution to the problem.

The design equations for the irrotational flow problem were programmed in FORTRAN IV. The computer program was used to carry out a parametric study to determine the optimum cowl lip radius and injection angle when the isometric constraint is one of fixed length. The resulting optimum nozzle was compared to one designed by Rao's method. The importance of the transonic flow analysis and the base pressure model are illustrated.

The primary advantages of the method developed here over that by Rao³ is that the present method can be extended directly to rotational and dissipative flows, and also a variety of geometric constraints are possible in lieu of the fixed length constraint.

References

¹ Guderley, G. and Hantsch, E., "Beste Formen für Achsensymmetrische Überschallschubdüsen," *Zeitschrift für Flugwissenschaften*, Vol. 3, 1955, pp. 305-313.

² Rao, G. V. R., "Exhaust Nozzle Contour for Optimum Thrust," *Jet Propulsion*, Vol. 28, 1958, pp. 377-382.

³ Rao, G. V. R., "Spike Nozzle Contour for Optimum Thrust," *Ballistic Missile and Space Technology*, Vol. 2, edited by C. W. Morrow, Pergamon Press, New York, 1961, pp. 92-101.

⁴ Guderley, K. G. and Armitage, J. V., "General Approach to Optimum Rocket Nozzles," *Theory of Optimum Aerodynamic Shapes*, edited by A. Miele, Academic Press, New York, 1965, Chap. 11.

⁵ Hoffman, J. D. and Thompson, H. D., "A General Method for Determining Optimum Thrust Nozzle Contours for Gas-Particle Flows," *AIAA Journal*, Vol. 5, No. 10, Oct. 1967, pp. 1886-1887.

⁶ Hoffman, J. D., "A General Method for Determining Optimum Thrust Nozzle Contours for Chemically Reacting Gas Flows," *AIAA Journal*, Vol. 5, No. 4, April 1967, pp. 670-676.

⁷ Hoffman, J. D., Scofield, M. P., and Thompson, H. D., "A Parametric Study of Boundary Layer Effects on Maximum Thrust Nozzle Contours," Rept. AFAPL TR-69-99, Oct. 1969, Air Force Aero Propulsion Lab., Wright-Patterson Air Force Base, Ohio.

⁸ Humphreys, R. P., Thompson, H. D., and Hoffman, J. D., "Design of Maximum Thrust Plug Nozzles for Fixed Inlet Geometry," Rept. 70-47, June 1970, Air Force Aero Propulsion Lab., Wright-Patterson Air Force Base, Ohio.

⁹ Rom, J., "Analysis of the Near-Wake Pressure in Supersonic Flow Using the Momentum Integral Method," *Journal of Spacecraft and Rockets*, Vol. 3, No. 10, Oct. 1966, pp. 1504-1509.

¹⁰ Moore, A. W. and Hall, I. M., "Transonic Flow in the Throat Region of an Annual Nozzle with an Arbitrary Smooth Profile," Rept. 26-543, Jan. 4, 1965, Aeronautical Research Council, London, England.

¹¹ Leipman, H. W. and Goddard, F. E., "Note on the Mach Number Effect Upon the Skin Friction of Rough Surfaces," *Journal of the Aeronautical Sciences*, Vol. 24, 1957, p. 784.

¹² Panov, I. A. and Shvets, A. I., "Investigation of the Base Pressure Near the Trailing Edge of Axisymmetric Bodies in Supersonic Flow," *Prikladnaya Mekhanika*, Vol. 2, No. 6, 1966, pp. 105-111.

Table 4 Coordinates of an optimum contour for the alternate base pressure model

x, in.	y, in.	θ° , deg
-0.56069	6.71874	-36.25027
-0.55023	6.71087	-37.75027
-0.53999	6.70272	-39.25027
-0.52996	6.69430	-40.75027
-0.52016	6.68563	-42.25027
-0.51059	6.67670	-43.75027
-0.49819	6.66442	-45.75027
-0.44272	6.60622	-46.29203
-0.33777	6.49721	-45.88483
-0.19453	6.35086	-45.35040
-0.00101	6.15730	-44.66440
0.34386	5.83114	-41.57284
0.90107	5.38449	-36.00408
1.72398	4.85222	-30.05107
2.55635	4.41335	-25.69669
3.61048	3.95442	-21.49032
4.92072	3.49325	-17.40459
6.53289	3.05192	-13.30646
8.49709	2.66542	-9.02277
11.58406	2.34099	-3.08106